Child's Nervous System (2019) 35:683–687
https://doi.org/10.1007/s00381-019-04103-5

ORIGINAL ARTICLE

Vertebral artery segment at the suboccipital dural penetration site: an anatomical study using magnetic resonance imaging

Satoshi Tsutsumi[1] · Hideo Ono[2] · Hisato Ishii[1] · Yukimasa Yasumoto[1]

Received: 4 February 2019 / Accepted: 20 February 2019 / Published online: 28 February 2019
© Springer-Verlag GmbH Germany, part of Springer Nature 2019

Abstract

Purpose The morphology of the vertebral artery (VA) segment at the suboccipital dural penetration site has little been explored with magnetic resonance imaging (MRI). Therefore, the aim of this study was to examine the structure using MRI.

Methods In total, 94 patients underwent thin-sliced, contrast MRI in the axial, coronal, and sagittal planes involving the atlas, axis, occipital bone, and V3 and V4 segments of the VA.

Results The VA segment at the suboccipital dural penetration site was well-delineated in 93% on the axial images and in 95% on the coronal images. The axial images showed that 82% of the VA penetration sites were located in the middle third of the dural sac. Meanwhile, the coronal images revealed that the heights of both VA penetration sites were located at the same level in 87%. The axial VA penetration angle, which is formed by the VA and tangential line of the dural sac, was 66 ± 11.9° on the right side and 61 ± 14.1° on the left side. The coronal VA penetration angle, which is formed by the tangential line of the VA and dural sac, was 111 ± 24.6° on the right side and 112 ± 19.9° on the left side.

Conclusions The morphology of the VA segment is considerably variable at the suboccipital dural penetration site, while most penetration sites are located in the middle third of the dural sac on axial MRI. These should be assumed during surgeries around the suboccipital VA penetration site.

Keywords Vertebral artery · Suboccipital · Dural penetration · MRI

Introduction

The V3 segment is a distinct part of the vertebral artery (VA). It presents a peculiar tortuous course from the exit of the transverse foramen of the axis to the penetration site of the suboccipital dura mater, variably giving rise to the posterior spinal artery and sending branches to the suboccipital muscles and dura mater [1, 3, 5, 6, 9, 10, 14, 15]. On the other hand, the incidence of V3 segment anomalies was low and found only in 0.77% of 1800 Caucasian patients [7]. Microscopic examinations have revealed that the thick dural layers formed at the VA penetration site function as peculiar structures not only to reinforce the adventitia of the VA but also to firmly anchor the VA to the suboccipital dura [11, 12]. In the clinical settings, the V3 segment has been a focus of attention because it is a predisposing site of dissecting aneurysm [4, 13]. Moreover, rotational VA compression at the dural penetration site can cause symptoms of vertebrobasilar insufficiency [2]. However, the morphology of the VA segment at the dural penetration site has little been explored with magnetic resonance imaging (MRI).

The present study aimed to characterize the VA segment at the dural penetration site using a contrast MRI.

Materials and methods

The present retrospective study included 94 patients who presented as outpatients to our hospital between April 2010

✉ Satoshi Tsutsumi
shotaro@juntendo-urayasu.jp

[1] Department of Neurological Surgery, Juntendo University Urayasu Hospital, 2-1-1 Tomioka, Urayasu, Chiba 279-0021, Japan

[2] Division of Radiological Technology, Medical Satellite Yaesu Clinic, Tokyo, Japan

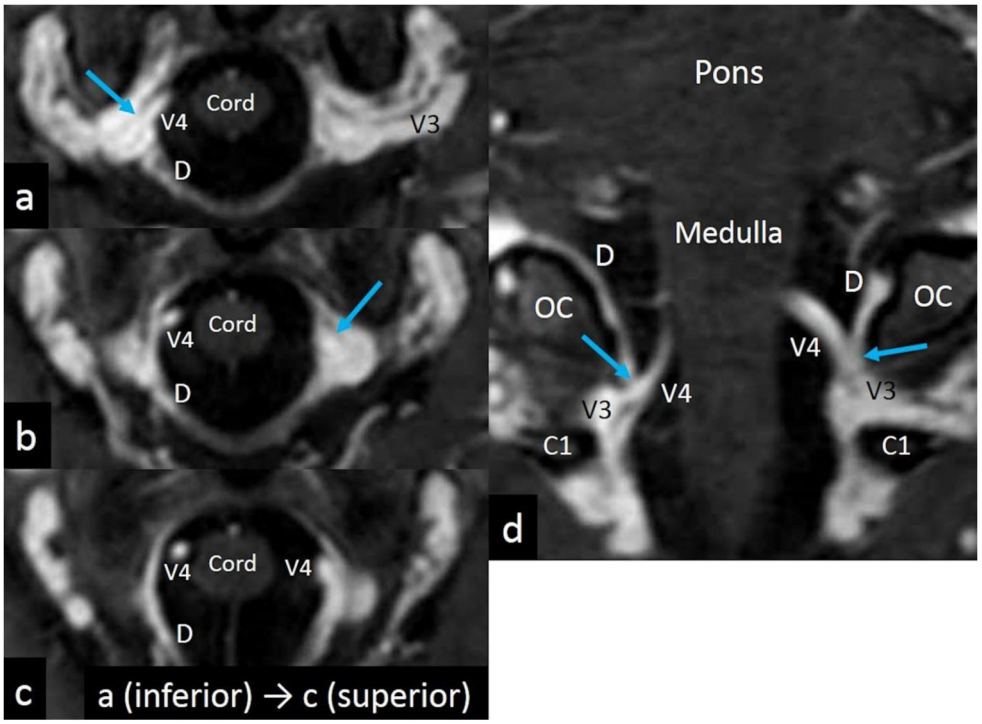

Fig. 1 Post-contrast consecutive axial (**a**-**c**) and coronal (**d**) magnetic resonance images of a 32-year-old woman showing the suboccipital dural penetration sites of the vertebral arteries on both sides. Note that on axial images, both penetration sites are located in the middle third of the dural sac (**a**, **b** arrow), while on a coronal image, the penetration site on the left side is higher than that on the right side (**d** arrows). C1 atlas, D dura mater, OC occipital condyle, V3 V3 segment of the vertebral artery, V4 V4 segment of the vertebral artery

and April 2016 and underwent MRI examinations. They presented with headaches, dizziness, tinnitus, hearing, and hemisensory disturbances, and seizures. Patients with a history of vertebrobasilar insufficiency, traumatic brain and spinal injuries, dissecting VA aneurysms, brain infarction in the distribution of the vertebrobasilar system, and surgeries in the craniocervical junction were excluded from the study. The patient population consisted of 41 men and 53 women with a median ± standard deviation age of 50 ± 16.2 years (range, 13–83 years). Initial examinations using axial T1-weighted and T2-weighted, T2 gradient echo, fluid-attenuated inversion recovery, and diffusion-weighted sequences confirmed that none of the patients had any signs of anomalies in the atlas, axis, and occipital bone. The patients then underwent imaging examination with intravenous gadolinium infusion (0.1 mmol/kg) in the axial, coronal, and sagittal planes involving the atlas, axis, occipital bone, and V3 and intracranial V4 segments of the VA. The following parameters were adopted: repetition time, 4.1 ms; echo time, 1.92 ms; slice thickness, 1 mm; interslice gap, 0 mm; matrix, 320 × 320; field of view, 250 mm; flip angle, 13°; and scan duration, 7 min 25 s. All imaging sequences were performed using a 3.0-T MRI scanner (Achieva R2.6; Philips Medical Systems, Best, The Netherlands). The VA segment at the suboccipital dural penetration site and its associated structures were assessed on axial and coronal images.

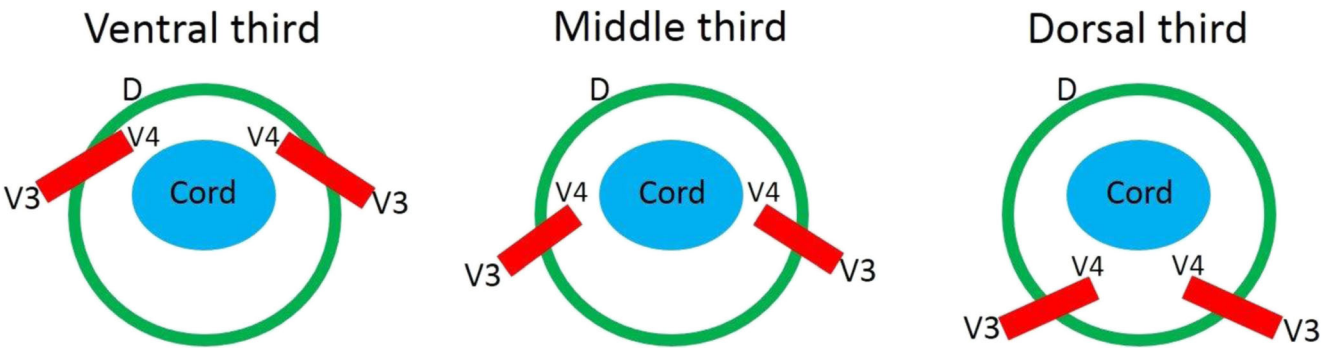

Fig. 2 Schematic drawings of post-contrast axial magnetic resonance images showing three different dural penetration sites of the vertebral artery at the ventral, middle, and dorsal third of the dural sac

Table 1 Distribution of dural penetration sites of the vertebral artery

Type	Distribution
Ventral third	18% (32/174)
Middle third	82% (142/174)
Dorsal third	0

Table 2 Types and distributions of heights of both dural penetration sites

Type	Distribution
A (R = L)	87% (77/89)
B (R > L)	2% (2/89)
C (R < L)	11% (10/89)

Imaging data were transferred to a workstation (Virtual Place Lexus 64. 64th edition; AZE, Tokyo, Japan) and independently analyzed by two authors (H.I. and H.O.).

The study was conducted in accordance with the guidelines of our institution regarding human research. Written informed consent was obtained from all patients prior to their participation in this study.

Results

The VA segment at the suboccipital dural penetration site was well-delineated bilaterally among 87 of the 94 patients (93%) on the axial images and among 89 of the 94 patients (95%) on the coronal images (Fig. 1). The remaining patients were excluded from the analysis because they had extremely hypoplastic VAs unilaterally or bilaterally, which were not amenable to reliable evaluation. On the axial images, the VA penetration site was classified into three locations: the ventral, middle, and dorsal third of the dural sac (Fig. 2). The middle third was the most predominant site and was found in 142 of the 174 sides (82%), followed by the ventral third in 32 sides (18%). The penetration site was not identified in the dorsal third (Table 1). On the coronal images, the heights of both VA penetration sites were classified into three types: types A, B, and C. In type A, both VA penetration sites were located at the same level of the dural sac, while in type B, the penetration site was higher on the right side. In type C, the penetration site was higher on the left side (Fig. 3). Type A was the most predominant type of height and found in 77 of the 89 patients (87%), followed by Type C in 10 patients (11%). Type B was the least predominant type of height and identified in 2 patients (2%) (Table 2). The VA penetration angle into the suboccipital dura mater was assessed on both axial and coronal images. On the axial images, the angle formed by the posterior margin of the VA and tangential line of the outer dural sac at the dural penetration site (1) was measured (Fig. 4a). The 1 calculated as the median ± standard deviation was 66 ± 11.9° on the right side and 61 ± 14.1° on the left side. Distribution of the 1 among 87 patients is summarized in Fig. 5. However, on the coronal images, the angle formed by the tangential line of the lower VA at the penetration site and inner dural sac (2) was measured (Fig. 4b). The 2 calculated as the median ± standard deviation was 111 ± 24.6° on the right side and 112 ± 19.9° on the left side. Distribution of the 2 among 89 patients is summarized in Fig. 6. The 1 and 2 were highly variable and commonly asymmetrical on both sides. In the present study, no anomalies were found in the V3 segments.

Discussion

In this study, the VA segment at the suboccipital dural penetration site was well-delineated in more than 90% of the 94 patients. The axial images showed that more than 80% of the

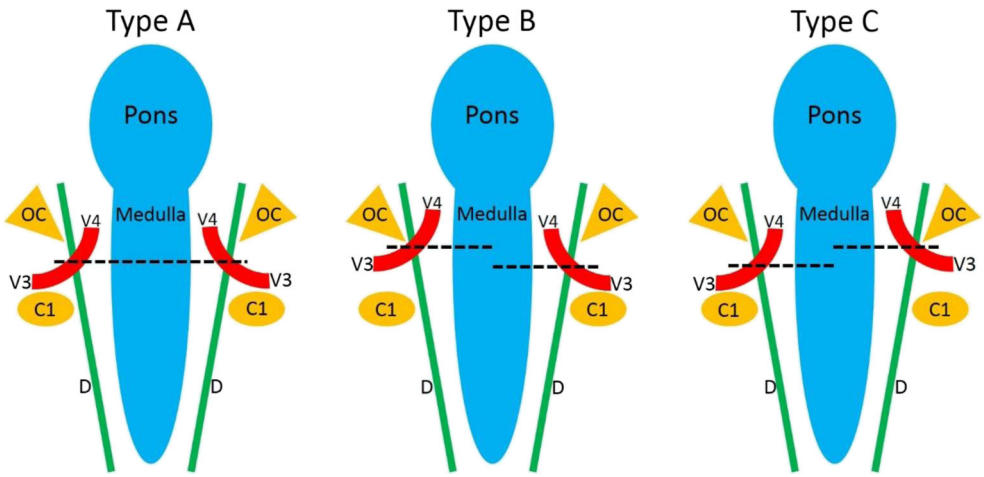

Fig. 3 Schematic drawings of post-contrast coronal magnetic resonance images showing three types of heights of both dural penetration sites. Type A: the same level of heights on both sides; Type B: higher on the right side; Type C: higher on the left side

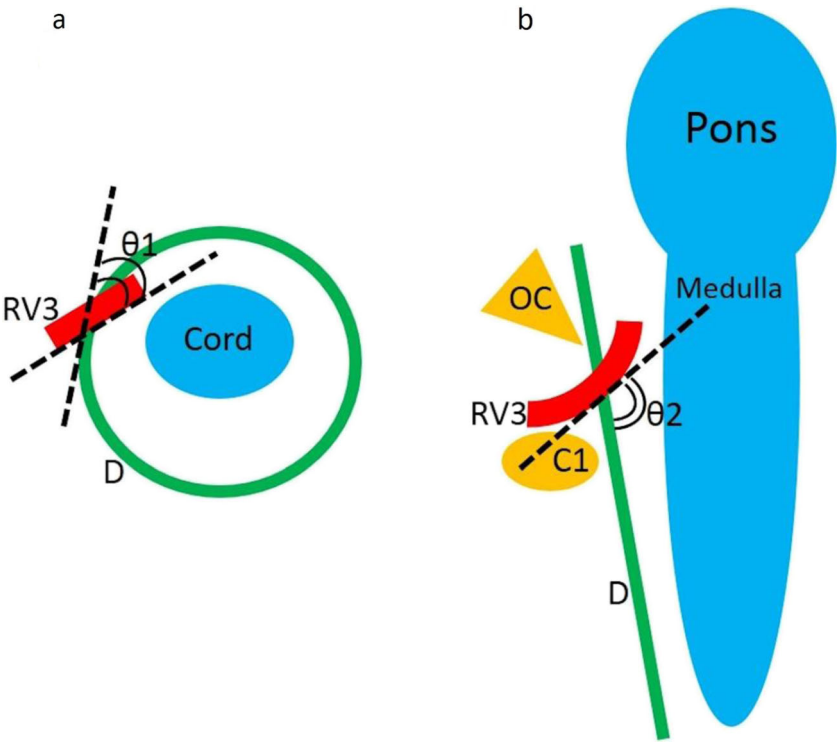

Fig. 4 Illustrations of the penetration angle of the vertebral artery into the suboccipital dura mater. Schematic drawings of post-contrast axial (**a**) and coronal (**b**) magnetic resonance images showing an angle formed by the posterior margin of the vertebral artery and tangential line of the outer surface of the dural sac at the dural penetration site (1) and an angle formed by the tangential line of the lower vertebral artery at the penetration site and inner surface of the dural sac (2). RV3 right V3 segment of the vertebral artery

VA penetration sites were located in the middle third of the dural sac. Meanwhile, the coronal images revealed that most of the bilateral VA penetration sites were located at the same level. To date, little is known on the development of VA segments around the craniocervical junction. A recent investigation documented that the VA takes a straight upward course at the craniocervical junction before 8–9 gestational weeks. At a later period, the atlanto-occipital joint growing along the mediolateral axis causes peculiar tortuous curves of the V3 segment at the junction area [8]. As the consistency of the VA penetration site found in the present study is contradictory with the common morphological variability of the VA at the craniocervical junction [1, 3, 5–7, 10, 14, 15], further verification using comprehensive approaches is necessary. In addition to the morphological characteristics based on the embryology, factors associated with variable motions of the cervical spine should be explored to understand the flow of the VA and etiology of dissecting VA aneurysm at the suboccipital dural penetration site [2]. On the other hand, the VA penetration angles into the suboccipital dural sac, which were assessed in the axial and coronal planes showed considerable interindividual variability and bilateral asymmetry. This may be associated with the interindividual differences in chronological changes of the topographical anatomy of the VA during the embryonic period [8].

The present study has limitations and weaknesses. The study population consisted of patients with inhomogeneous

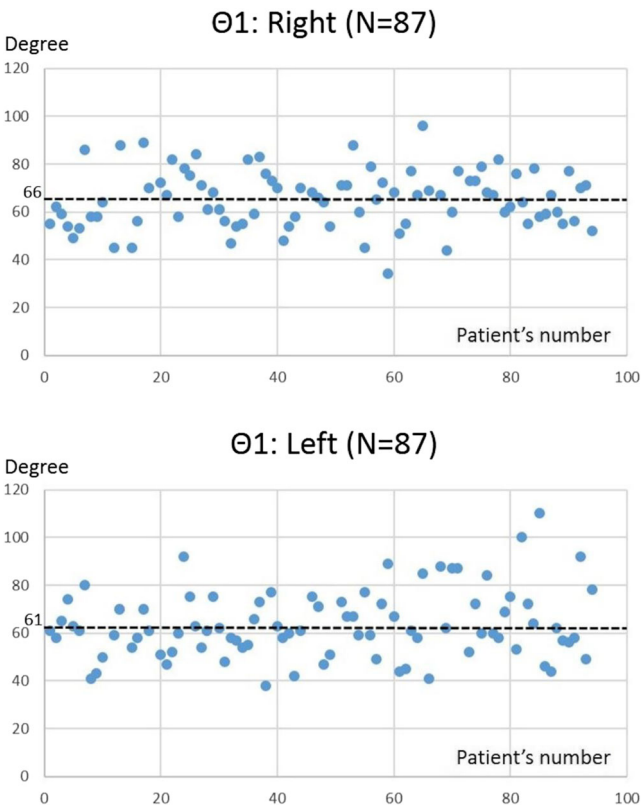

Fig. 5 Distribution of the 1 on both sides. Dotted line: median value

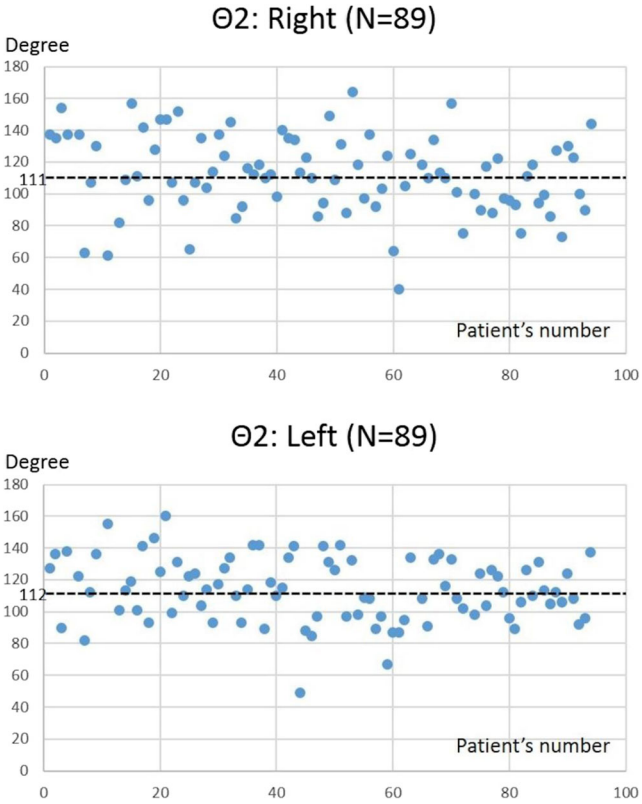

Fig. 6 Distribution of the 2 on both sides. Dotted line: median value

age distribution and uneven gender ratio. They were retrospectively evaluated and not randomly assigned to the MRI examinations. Furthermore, the VA, paravertebral venous plexus, and dura mater were not completely differentiated using the resolution of the adopted MRI, although it did not disturb an objective evaluation. Despite these limitations, however, we believe that the results of this study provide a better understanding of the morphology of the VA segment at the suboccipital dural penetration site.

Conclusions

The morphology of the VA segment is considerably variable at the suboccipital dura penetration site, while most penetration sites are located in the middle third of the dural sac on the axial MRI. These should be assumed during surgeries around the suboccipital VA penetration site.

Author contributions ST conceptualized the project of the study.
HI and YY collected the imaging data.
HO and HI analyzed the imaging data.
ST wrote the manuscript.

Compliance with ethical standards

Conflict of interest The authors declare that they have no conflict of interest.

Publisher's note Springer Nature remains neutral with regard to jurisdictional claims in published maps and institutional affiliations.

References

1. Abd el-Bary TH, Dujovny M, Ausman JI (1995) Microsurgical anatomy of the atlantal part of the vertebral artery. Surg Neurol 44(4):392–401
2. Akar Z, Kafadar AM, Tanriover N, Dashti RS, Islak C, Kocer N, Kuday C (2000) Rotational compression of the vertebral artery at the point of dural penetration. Case report J Neurosurg 93(2 Suppl): 300–303
3. Arnautović KI, al-Mefty O, Pait TG, Krisht AF, Husain MM (1997) The suboccipital cavernous sinus. J Neurosurg 86(2):252–262
4. Arnold M, Bousser MG, Fahrni G, Fischer U, Georgiadis D, Gandjour J, Benninger D, Sturzenegger M, Mattle HP, Baumgartner RW (2006) Vertebral artery dissection: presenting findings and predictors of outcome. Stroke 37(10):2499–2503
5. Cengiz SL, Cicekcibasi A, Kiresi D, Kocaogullar Y, Cicek O, Baysefer A, Buyukmumcu M (2009) Anatomic and radiologic analysis of the atlantal part of the vertebral artery. J Clin Neurosci 16(5):675–678
6. Duan S, Lv S, Ye F, Lin Q (2009) Imaging anatomy and variation of vertebral artery and bone structure at craniocervical junction. Eur Spine 18(8):1102–1108
7. Fortuniak J, Bobeff E, Polguj M, Kośla K, Stefańczyk L, Jascólski DJ (2016) Anatomical anomalies of the V3 segment of the vertebral artery in the Polish population. Eur Spine 25(12):4164–4170
8. Ha YS, Cho KH, Abe S, Abe H, Rodriguez-Vázquez JF, Murakami G (2013) Early development of the human vertebral artery especially at and above the occipitovertebral junction. Surg Radiol Anat 35(9):765–773
9. Kim KS (2016) Developmental anomalies of the distal vertebral artery and posterior inferior cerebellar artery: diagnosis by CT angiography and literature review. Surg Radiol Anat 38(9):997–1006
10. Kiresi D, Gumus S, Cengiz SL, Cicekcibasi A (2009) The morphometric analysis of the V2 and V3 segments of the vertebral artery: normal values on MDCT. Comput Med Imaging Graph 33(5):399–407
11. Peltier J, Toussaint P, Deramond H, Gondry C, Bruniau A, Gontier MF, Le Gars D (2003) The dural crossing of the vertebral artery. Surg Radiol Anat 25(3–4):305–310
12. Piffer CR, Zorzetto NL (1980) Microscopy anatomy of the vertebral artery in the suboccipital and intracranial segments. Anat Anz 147(4):382–388
13. Provenzale JM, Morgenlander JC, Gress D (1996) Spontaneous vertebral dissection; clinical, conventions angiographic, CT and MR findings. J Comput Assist Tomogr 20(2):185–193
14. Rojas S, Ortega M, RodríGuez-Baeza A (2018) Variable anatomic configuration of the posterior spinal arteries in humans. Clin Anat 31(8):1137–1143
15. Tubbs RS, Shah NA, Sullivan BP, Marchase ND, Cohen-Gadol AA (2009) Surgical anatomy and quantitation of the branches of the V2 and V3 segments of the vertebral artery. Laboratory investigation. J Neurosurg Spine 11(1):84–87